Scientific African 16 (2022) e01152

Contents lists available at ScienceDirect

Scientific African

journal homepage: www.elsevier.com/locate/sciaf

Green synthesis of zinc oxide nanoparticles using plantain peel extracts and the evaluation of their antibacterial activity

Emmanuel E. Imade[a], Timothy O. Ajiboye[b,c], Ayomide E. Fadiji[d], Damian C. Onwudiwe[b,c,*], Olubukola O. Babalola[d]

[a] Department of Microbiology, Faculty of Life Sciences, University of Benin, Private Mail Bag 1154, Benin City, Edo State, Nigeria
[b] Material Science Innovation and Modelling (MaSIM) Research Focus Area, Faculty of Natural and Agricultural Sciences, North-West University, Mafikeng Campus, Private Bag X2046, Mmabatho 2735, South Africa
[c] Department of Chemistry, School of Physical and Chemical Sciences, Faculty of Natural and Agricultural Sciences, North-West University, Mafikeng Campus, Private Bag X2046, Mmabatho 2735, South Africa
[d] Food Security and Safety Focus Area, Faculty of Natural and Agricultural Sciences, North-West University, Private Bag X2046, Mmabatho 2735, South Africa

ARTICLE INFO

Article history:
Received 27 December 2021
Revised 28 February 2022
Accepted 15 March 2022

Editor: DR B Gyampoh

Keywords:
Zinc oxide
Green synthesis
Antimicrobial
Plantain peels
Antibiotics resistance

ABSTRACT

The synthesis of nanoparticles via the green routes is an established technology for producing nano dimensional materials that are useful in different fields where environmental friendly materials are a major requirement. The present study reports a cost effective, eco-friendly and straightforward approach to synthesize zinc oxide nanoparticles (ZnONPs) using plantain peel extract. The optical, structural and morphological characteristics of the ZnONPs were studied using different techniques. X-ray diffraction analysis confirmed a hexagonal wurtzite structure, whose morphology and particle size, according to the transmission electron microscopy (TEM), was spherical and about 20 nm in size. The antimicrobial potency of the ZnONPs was evaluated using agar well diffusion and broth dilution assays against pathogenic strains of Salmonella enterica, *Klebsiella pneumoniae*, *Bacillus cereus* MTCC 430 and *Staphylococcus aureus* 26923, isolated from beef. The biosynthesized ZnONPs demonstrated good antimicrobial activity with a MIC value of 100 µg/mL for all the test isolates. Based on the results obtained, the antimicrobial efficacy of the nanoparticles against the selected bacteria followed the sequence: *S. aureus* > *B. cereus* > *K. pneumoniae* > *S. enterica*. The results showed that plantain peels, which are the waste of these fruits, could be helpful for the green synthesis of ZnONPs with good antibacterial efficacy.

Introduction

The menace of foodborne infections has become a major global public health concern. According to the World Health Organization (WHO), foodborne infections impact over 30% of the population in developed nations each year. The main

* Corresponding author at: Material Science Innovation and Modelling (MaSIM) Research Focus Area, Faculty of Natural and Agricultural Sciences, North-West University, Mafikeng Campus, Private Bag X2046, Mmabatho 2735, South Africa.
E-mail address: nwudiwe@nwu.ac.za (D.C. Onwudiwe).

https://doi.org/10.1016/j.sciaf.2022.e01152

source of foodborne illness in humans is the intake of foods contaminated with foodborne pathogens such as bacteria, fungi, viruses, and toxins. During pre-harvesting, post-harvesting, processing, transport, handling, or preparation, food, especially poorly processed food, can be contaminated [1]. Some common pathogens found in food are *Salmonella, Klebsiella, Staphylococcus, and Bacillus spp* [2–4]. Control of pathogens is a critical aspect of public health, especially with respect to foodborne diseases [5, 6]. The use of antibiotics and other methods currently engaged in controlling pathogens have been limited by economic factors and the incidence of resistance of pathogens to antibiotics. Allen et al [7]. reported that the current distribution of antibiotic resistance genes into pathogenic bacteria questions the efficacy of today's antibiotic repertoire in the near future. This has been exacerbated by the widespread antibiotic use and antibacterial pharmacokinetics, such as maintaining insufficient bactericidal concentrations at the infection site. Furthermore, the practice of self-medication, blatant flouting of recommended doses and frequent use, influence the development of bacterial resistance to antibiotics [8]. This has resulted in the emergence of super-bacteria which are resistant to nearly all antibiotics [9]. The majority of antibiotic resistance mechanisms are irrelevant for nanoparticles (NPs) because their method of action is direct contact with the bacterial cell wall, rather than penetration.

The production, manipulation and use of materials below 100 nm range is known as Nanotechnology [10, 11]. Nanoparticles (NPs) can be synthesized using three major methods, including physical, chemical and biological methods. The chemical method is the conventional and most employed method [12]; however, the disadvantage of this process, is the possibility of synthesising materials that could be toxic to cells [13]. Consequently, there is a drift towards the synthesis of NPs by using extracts of plants, which are less toxic. Also worthy of note is the fact that, plants contain active pharmacological ingredients, which can intensify the biomedical efficacy of NPs by serving as capping and reducing agents [14]. This helps to reduce the amount of raw materials required for synthesis and promotes green technologies. In addition, plant-mediated nanoparticles synthesis is preferred because it is eco-friendly, energy-efficient, cost-effective, safe for human therapeutic use and involves a single-step process for biosynthesis [15, 16].

Green biotechnology is geared towards designing biochemical products and processes that reduce or eliminate the application or generation of hazardous substances that adversely affects the environment and human health. Recent studies have established that plants parts such as leaves, fruits, seeds and fruit peels are rich sources of bioactive compounds if extracted efficiently [17]. One of such is plantain peel (Musa paradisiaca). It is an herbaceous, perennial, monocotyledonous plant [18] belonging to the genus Musa along with (dessert) bananas (M. sapientum) in the family Musacaceae [19, 20]. Musa paradisiaca is a tropical tree-like herb [21] that can grow as high as 3–15 m with an aerial pseudostem and submerged rhizome, which produces the large, pulpy, and starchy fruit (plantain) [22]. Consumption of plantain fruit comes with health benefits such as reduction of cholesterol, prevention of anaemia and treatment of stomach ulcers. It is also beneficial in pregnancy, diabetes, and as a weaning food for babies. The health benefits of this plant is not limited to the fruit alone, the peel contains phytochemicals such as tannins (28.4 mg/100 g), saponin (327 mg/100 g), phenols (89.4 mg/100 g) and flavonoids (1.0 mg/100 g) [20]. Plants produce phytochemicals (biocontrol agents) in order to prevent the proliferation of plant pathogens [23], and this has motivated several studies that focus on plant-derived compounds, as potentially bioactive substances against pathogens.

The aim of this study was to synthesize zinc oxide nanoparticles using plantain peel extract, characterization of the synthesized nanoparticles and evaluation of their antimicrobial activity against representatives of Gram-positive and Gram-negative human pathogenic microorganisms. The formation of the nanoparticles was examined by the use of UV–vis spectroscopy while the size and shape of the nanoparticles were determined using transmission electron microscopy (TEM).

Materials and methods

Collection and preparation of plantain peel extract

Musa paradisiaca was obtained from Food Lover's Market Mega City, Mmabatho, South Africa and identified accordingly. The peel was removed and washed with clean water to remove impurities and chopped into smaller bits. 1000 mL of distilled water was added to 464 g of the plantain peel and was blended using Bennet read blender model BRNPL10001, P.R.C. This was then filtered using a muslin cloth and allowed to stand to obtain a clear supernatant. The supernatant obtained was further filtered using Whatman No 1 filter paper, with a pore size of 25 µm. The extract was labelled plantain peel extract (PPE) and stored in a refrigerator for further studies.

Synthesis of zinc oxide nanoparticles (ZnONPs)

The ZnONPs were prepared using the clear supernatant of PPE. A solution of 4.4 g of zinc acetate ($ZnC_4H_6O_4$) in 10 mL of distilled water was added to 10 mL of the PPE, and the pH of the solution was adjusted to 12 using NaOH after which the solution was stirred on a magnetic stirrer at 85 °C. After 2 h, the particles were separated by centrifugation at 5500 rpm for 15 min, the supernatant was decanted while ethanol was added to remove impurities and centrifuged again under the same condition. The pellet was obtained in a clean crucible, dried in the oven for 8 h at 90 °C and thereafter calcinated at 350 °C for 2 h to obtain the sample labelled as ZnONPs.

Characterization of synthesized zinc oxide nanoparticles

The absorption spectrum of the ZnONPs was recorded using UV–vis spectrophotometer (UV-1901 Agilent Technology, Cary series UV–vis spectrometer, USA) set at a resolution of 0.5 nm. The functional groups present in the peel extract were confirmed using Bruker alpha-P FTIR spectrometer operated in the range of 4000–400 cm^{-1}. The powder X-ray diffraction (p-XRD) patterns of the nanoparticles were recorded on an automated Rontgen PW3040/60 X'Pert Pro-X-ray diffractometer operated at a scanning rate of 2^0 min^{-1} at 40 kV and 30 mA from 25 to 80^0 using a nickel-filtered Cu ($\lambda = 1.542$ Å) at room temperature. The morphological properties of the nanoparticles were determined using a model JEOL2100 transmission electron microscope (TEM) instrument fitted with a LaB 6 electron gun at an acceleration voltage of 30 kV at room temperature.

Antimicrobial assay of ZnONPs

The antimicrobial activities of the ZnONPs was assessed by agar well diffusion method against pure bacterial cultures isolated from beef. The test microorganisms were *Salmonella enterica, Klebsiella pneumoniae, Bacillus cereus* MTCC 430 and *Staphylococcus aureus* 26923. These microorganisms were swabbed uniformly on nutrient agar plates using sterile hockey stick. Five wells of 6 mm diameter were made using sterile cork borer. Different concentrations (5, 10, and 20 mg/mL) of ZnONPs solutions (20 μL) was poured into the corresponding wells with one well containing dimethylsulfoxide (DMSO)to serve as control. The solvents used for this assay were water and DMSO. After incubation at 35 $\pm$ 2 °C for 24–48 h, the plates were examined for the presence of inhibition zones. Inhibition was considered positive when the width of the clear zone around the wells was 0.5 mm or larger.

Preparation of varying concentration of nanoparticles suspension

Determination of% of inhibition and minimum inhibitory concentration (MIC)

The MIC was determined by preparing the ZnONPs-DMSO solution in vitro at increasing concentrations. An inoculum of 25 µL was pipetted from a 24 h broth culture of the various test organisms into 5 test tubes containing 50 mL of nutrient broth. The same amount (25 µL), but different concentrations of the nanomaterial was also pipetted into each test tube. In place of the nanomaterial, DMSO, which was used as the solvent, was pipetted into the first test tube, which served as the control. After incubating in a shaker incubator at 37 °C and 150 RPM for 16–20 h, the turbidity was measured at a wavelength of 600 nm using a spectrophotometer (Thermospectronic, Model Helios Epsilon, made in USA). Percentage of inhibition were calculated from the readings obtained from the spectrophotometer using the formula below.

$$\frac{Percentage of inhibition = Absorbance of control - Absorbance of sample}{Absorbance\ of\ control} X100$$

Results and discussion

The chemistry and synthesis of zinc oxide nanoparticles (ZnONPs)

The mechanism of the green synthesis of ZnO nanoparticles is presented in scheme 1. The plantain extract contains phytochemicals, which may vary according to different parts of the fruit. Hence, the composition significantly affects the nanoparticle synthesis. These phytochemicals are antioxidants and toxic-free chemicals. Hence, act as stabilising agents and are also able to convert the metal precursors to metal oxide nanoparticles, thereby act as both reducing and stabilizing agents [24]. The formation of the ZnO nanoparticles proceeds via a two-step process involving the formation of the hydroxide by the interaction of the zinc salt and the extract of plantain peels, and a calcination reaction at 350 °C to yield ZnO. Due to the attachment of Zn to the acetate anion, in the precursor salt, there is a high reduction potential and tendency to donate electrons. As a result of this, the Zn cation is easily coordinated to the different antioxidants present in the PPE through the OH group resulting in the formation of $Zn(OH)_2$ and an off white precipitate began to emerge. The formed $Zn(OH)_2$ is then followed with calcination process to give ZnO as presented in Scheme 1 [25,26].

Identification, isolation, and mass synthesis of bioactive compounds against pathogens are required for the management of foodborne diseases. ZnO nanoparticles exhibit high antibacterial efficacy at concentrations as low as (0.16–5.00 mmol/L), either by disruption of the cell membrane [27], generation of reactive oxygen species (ROS) [28], hindering bacterial DNA amplification, or down-regulation of gene expression [29]. Obtaining these nanoparticles from plant extracts gives an added advantage because they serve as reducing agents and surfactants by binding to the metal ions to form the respective hydroxide. The formation of the metal oxide involves calcination, a thermal process, which determines the structure, size and crystalline nature of the synthesized nano-materials. The stages involved in the synthesis of ZnONPs from PPE are represented in Fig. 1.

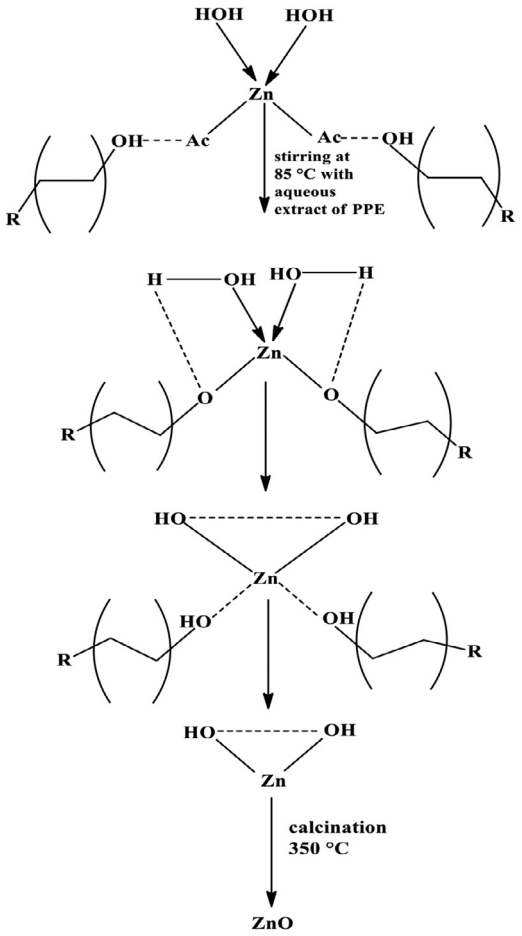

Scheme 1. Proposed mechanism for PPE mediated synthesis of ZnO nanoparticles. Note ⟨⟩R is organic components of PPE.

X-Ray diffraction (XRD) pattern of ZnO nanoparticle

Fig. 2 is the XRD pattern of ZnO nanoparticles after calcination at 350 °C for 2 h. The definite broadening of the XRD peaks indicate that the analysed sample contains particles in nanoscale range. Position and width, peak intensity and full-width at half-maximum (FWHM) were determined from the XRD patterns analysis. The diffraction peaks located at 31.84, 34.52, 36.33, 47.63, 56.71, 62.96, 68.13,69.18,72.61 and 77.11 are indexed to (100), (002), (101), (110), (103), (200), (112), (201), (004) and (202) respectively of a hexagonal wurtzite phase of ZnO [30] with lattice constants $a = b = 0.324$ nm and $c = 0.521$ nm (JPCDS card number: 36-1451) [31]. Furthermore, it was also confirmed that the synthesized nanopowder was free of impurities because it did not contain any other XRD peaks besides that of ZnO [32]. The diameter of the synthesized ZnO nanoparticle was estimated using Debye-Scherrer formula (Eq. (1))

$$D = K\lambda/\beta \cos\theta \tag{1}$$

where $K = 0.9$ is the shape factor, γ is the wavelength of X-ray used (1.5406 A), θ is the Bragg diffraction angle, and β is the full width at half maximum (FWHM).

The estimated crystallite size of the ZnONPs was about 18.06 nm and this was in the range of the values obtained in previous similar studies [32].

Optical characterization

UV–visible absorption and emission spectrum studies

The UV–visible spectrum of the synthesized nanoparticles in absolute ethanol is shown in Fig. 3a, and clearly shows that the maximum absorption peak appears at 378 nm which has also been reported for ZnONPs with a hexagonal wurtzite structure [33]. The optical band gap energy of the zinc oxide at the maximum absorption peak was obtained from Eq. (2) as

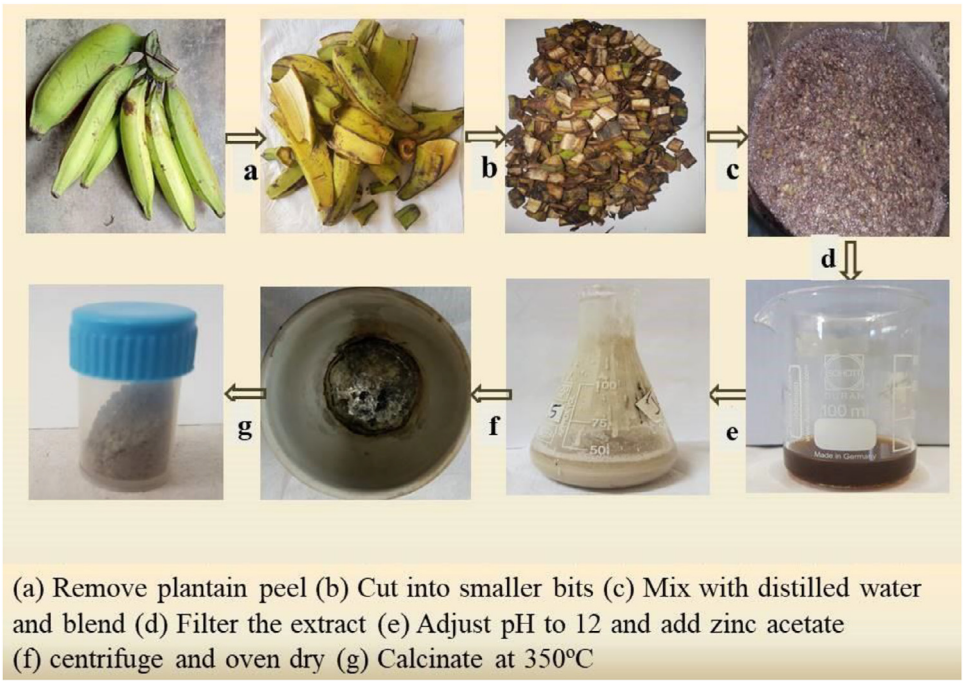

Fig. 1. Pictorial representation of steps involved in the green synthesis of ZnONP using plantain peel extract (PPE).

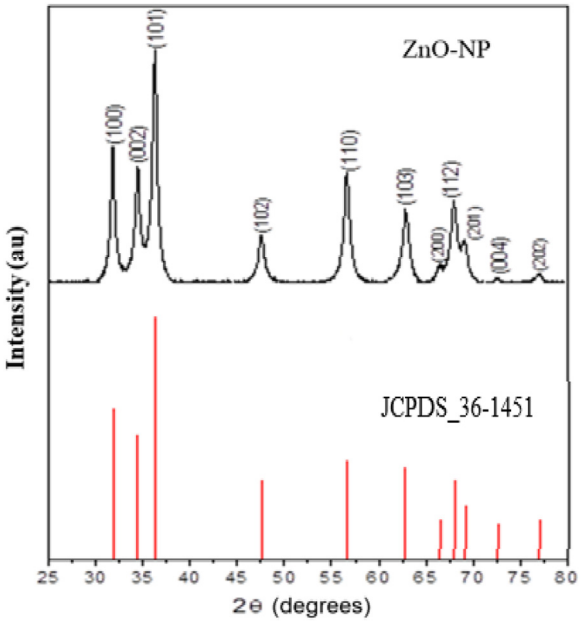

Fig. 2. XRD pattern of ZnO nanoparticles synthesized from peel extract of Musa paradisiaca.

3.28 eV.

$$E_g = h\nu/\lambda = 1240/\lambda \tag{2}$$

Where γ= wavelength of maximum absorption; h= Planck's constant, c=speed of light

In addition to the optical band gap at the wavelength of maximum absorption, the band gap of the synthesized ZnONP was also estimated from Tauc equation and Tauc plot shown in Eq. (3) and Fig. 3(b) respectively.

$$\propto h\nu = D(h\nu - E)^n \tag{3}$$

Where $h\nu$= photon's energy of the incident radiation; E_g = band gap of the synthesized material; D and n are constant.

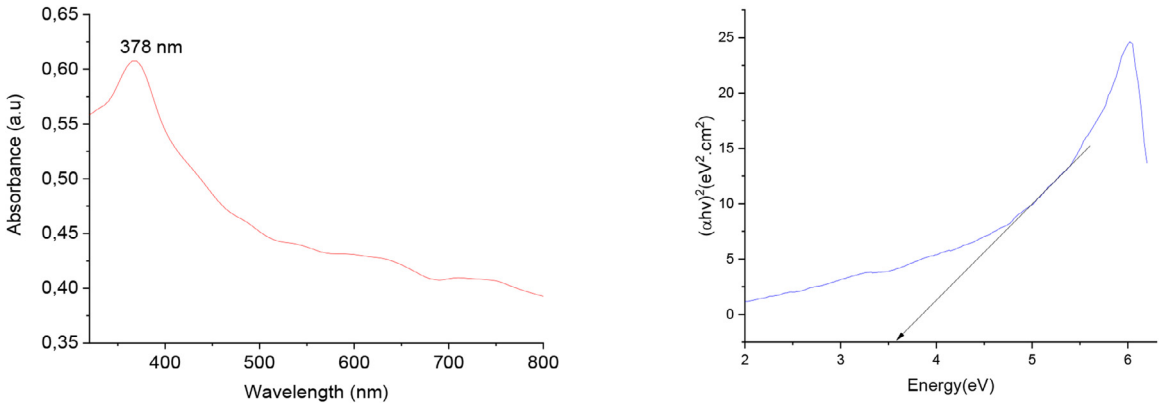

Fig. 3. (a) UV–vis spectrum of the synthesized zinc oxide (b) Tauc plot of synthesized zinc oxide.

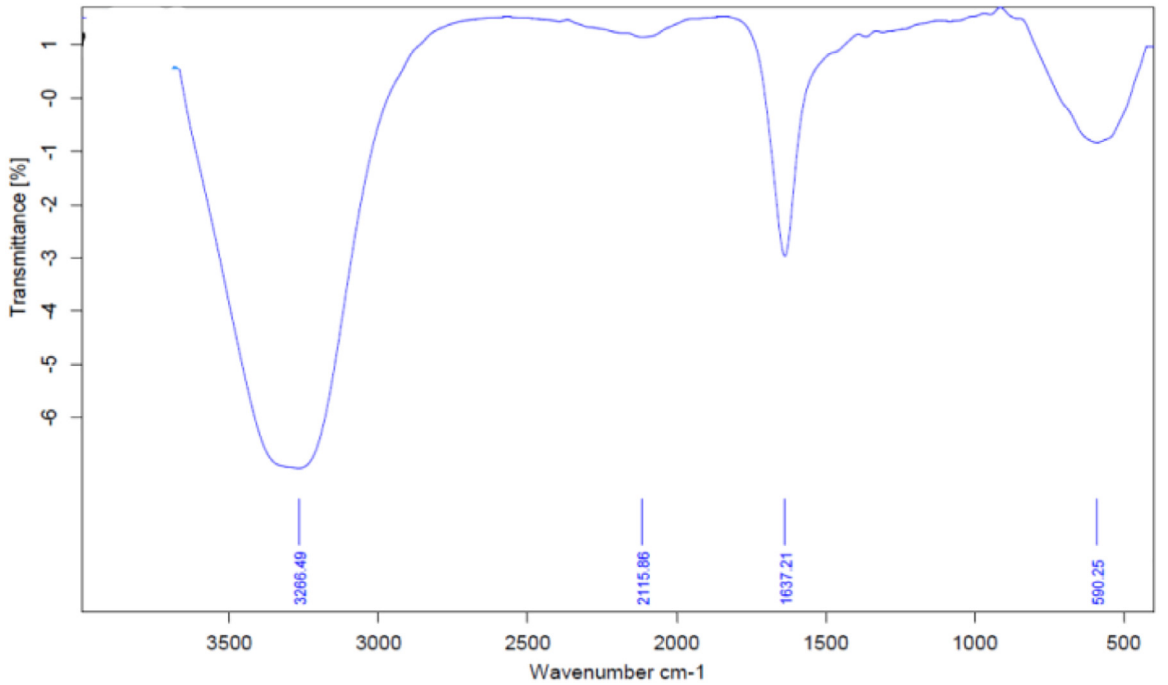

Fig. 4. FTIR spectrum of unripe plantain peel extract.

The Tauc plot was obtained from this equation by plotting $(\propto h\nu)^2$ against $h\nu$ while the bandgap of 3.65 eV was obtained by extrapolating the linear part of the plot to the energy ($^{h\nu}$) axis. The higher value of bandgap compared to that of the bulk is due to quantum confinement effect [31].

Fourier transform infrared spectroscopy (FTIR)

The plantain peel has been previously reported to contain biogenic amines, phenolic compounds and carotenoids [22]. Some of the functional groups that are present in the extract of plantain peel emanated from these compounds. The FTIR spectrum (Fig. 4) shows the presence of aromatic C–H out of plane vibration at 590.25 cm^{-1} and the peaks at 1636.71 and 3296.07 cm^{-1} are the bending and stretching vibrations of the O–H respectively [34]. This indicated the presence of hydroxyl compounds in the plantain peel extract.

Morphological studies and chemical analysis

The size, morphology and surface area of nanoparticles play important roles in their properties and characteristics. The morphological, size, and compositional analysis of the ZnO NPs were studied by TEM, SEM and EDX as presented in Fig. 5.

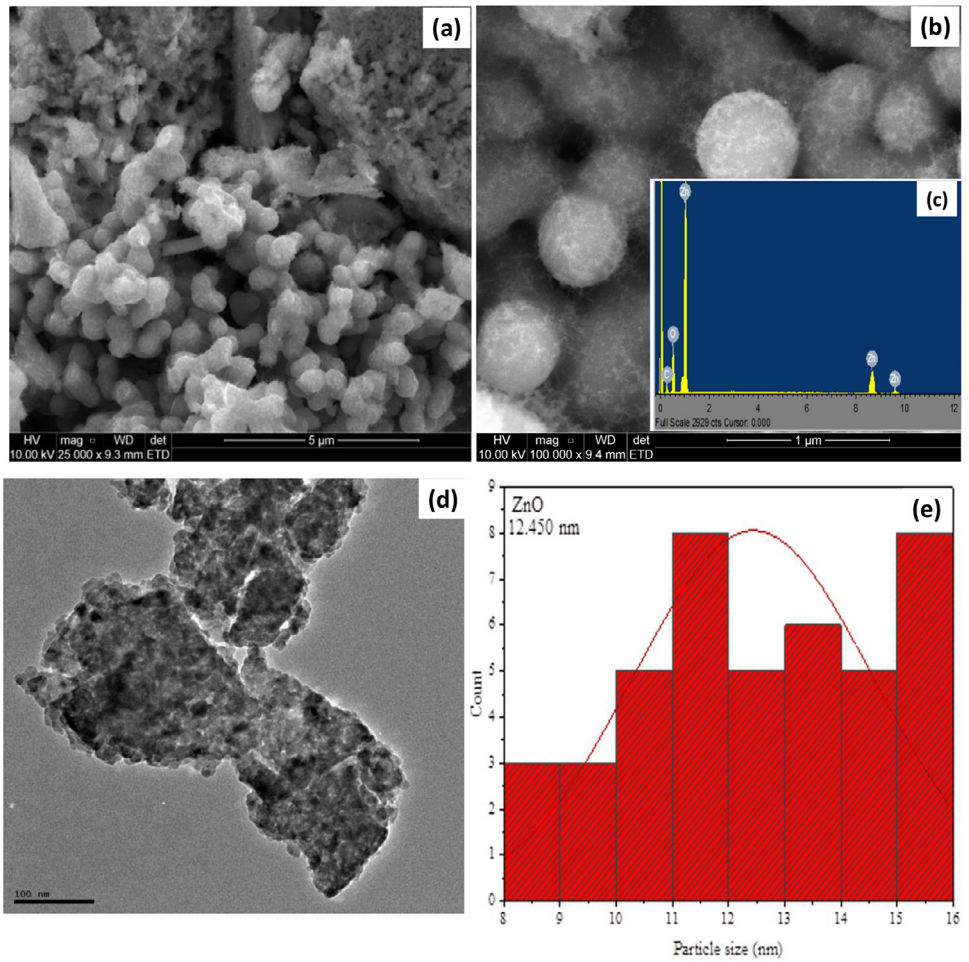

Fig. 5. SEM images at (a) low magnification, (b) high magnification, (c) EDS spectrum as inset, (d) TEM image, and (d) particle size distribution histogram of the synthesized ZnO nanoparticles.

The SEM micrograph (Fig. 5a) indicated that the ZnONPs were of spherical morphology, with smooth surface and good distribution across the surface as shown in the higher magnification images of Fig. 5b. EDX result shown in the inset of Fig. 5b reveals a single peak of O identified at 0.5 KeV, and three peaks of Zn identified at 1, 8.4 and 9.8 KeV. These peaks characteristic of only Zn and O elements, without any additional peaks, confirmed the purity of the biosynthesized ZnONPs. This also corroborates with the results obtained from both the XRD and FTIR analyses. The internal morphology presented by the TEM images of Fig. 5d showed spherical morphology with slight agglomeration typical of particles prepared via a calcination process. An average particle size of 12.45 nm was obtained from the particle size distribution histogram obtained using the origin software (Fig. 5e). The size is in good agreement with the results obtained from the XRD analysis.

Antimicrobial susceptibility assay

The antimicrobial efficacy of the ZnONPs was investigated on four food-borne pathogenic organisms (*S. enterica*, *K. pneumonia*, *S. aureus* and *Bacillus cereus*) using the agar well diffusion and agar broth dilution methods Fig. 6. shows the magnitude of the susceptibility of the various pathogenic organisms.

The diameter of the zone of inhibition (ZOI) varied for the different organisms. The highest ZOI was recorded in the treatment against *S. aureus* ATCC 26923, while *K. pneumoniae* demonstrated the lowest ZOI. This was similar to the reports of Chennimalai [35], where *Bacillus cereus*, a Gram-positive bacterium was observed to be more sensitive to ZnO nanocrystals compared to Gram-negative pathogens. The mean of three replicates of the diameter of ZOI (in millimeters) induced by the ZnONPs suspension is presented in Table. 1.Table. 2 Table. 3..

This green synthesized ZnONPs exhibited a high degree of antimicrobial activity against Gram-positive bacteria. One major function of the bacterial cell walls and membrane is for protection against environmental threats. Therefore, bacteria are classified based on the differences in the cell wall structures. Gram-negative cell wall, which is also referred to as

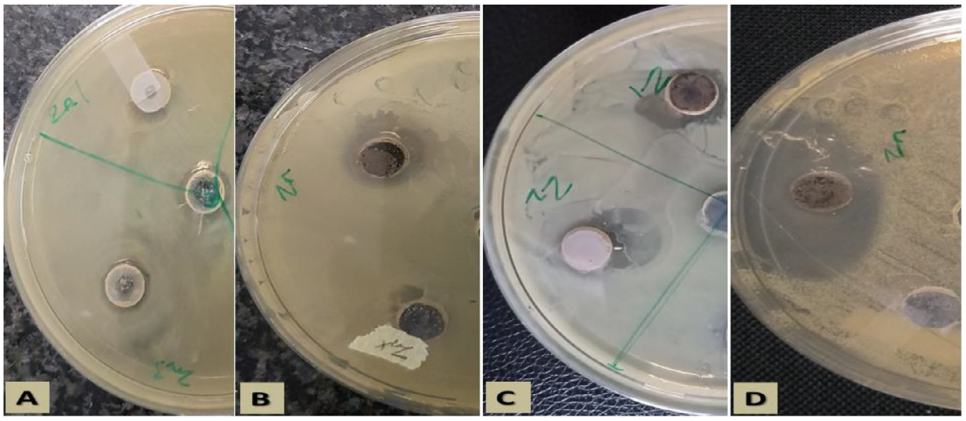

Fig. 6. Zone of inhibition of green synthesized ZnONPs against (A) K. pneumoniae (B) B. cereus (C) S. enterica (D) S. aureus ATCC 26923.

Table 1
Mean width of inhibition zone (in millimeters) induced by the ZnONPs.

S/N	Organism	Mean width of Inhibition Zone (mm)
1	*Salmonella enterica*	10.67 ± 0.58
2	*Klebsiella pneumoniae*	12.00 ± 1.00
3	*Staphylococcus aureus*	27.67 ± 6.81
4	*Bacillus cereus*	12.00 ± 1.73

Table 2
Optical density reading of broth culture at 600 nm.

S/N	Test isolate	Concentration of ZnONPs					
		0 µg/ml	10 µg/mL	100 µg/mL	500 µg/mL	1000 µg/mL	5000 µg/mL
1	*Salmonella enterica*	1.403	1.408	1.097	1.046	1.022	1.019
2	*Klebsiella pneumoniae*	1.225	1.230	1.035	0.861	0.836	0.798
5	*Staphylococcus aureus*	1.371	1.374	0.998	0.957	0.940	0.938
6	*Bacillus cereus*	1.337	1.339	1.087	1.044	1.036	1.021

Table 3
Percentage of inhibition and Minimum Inhibitory Concentration (MIC) of ZnONPs.

S/N	Test isolate	Percentage of inhibition (%)				
		10 µg/ml	100 µg/ml	500 µg/ml	1000 µg/ml	5000 µg/ml
1	*Salmonella enterica*	0.00	21.81	65.75	67.46	61.76
2	*Klebsiella pneumoniae*	0.00	15.51	29.71	31.76	34.86
5	*Staphylococcus aureus*	0.00	27.21	30.20	31.44	31.58
6	*Bacillus cereus*	0.00	18.70	21.91	22.51	23.64

cell envelope, basically contains two layers of lipopolysaccharides. In contrast, Gram-positive cell wall is typically thicker and primarily composed of a single type of molecule, peptidoglycans. Roy et al [36]. reported that most ZnONPs show higher antibacterial activity against Gram-negative bacteria than Gram-positive bacteria, due to the natural barrier that Gram-positive bacterial cell wall provides. Consequently, the ZnONPs synthesized in this study is of utmost value as it demonstrates high degree of antimicrobial activity against Gram-positive bacteria, thereby making it a good therapeutic agent against Gram-positive pathogenic bacteria.

Minimum inhibitory concentrations (MICs) are the lowest antimicrobial concentrations that will inhibit visible microorganism growth after an overnight incubation period. The notion of minimum inhibitory concentration was developed by Alexander Fleming, who used the turbidity of broth to measure the antibacterial effectiveness of medicines. The Clinical and Laboratory Standards Association combined methodologies and standards for MIC determination and clinical application for antibiotic bacteriostatic effects evaluation in the late 1980s. In microbiology, the minimum inhibitory concentration (MIC) is the lowest concentration of chemicals (usually drugs) that prevent the visible growth of bacteria. The MIC depends on the microorganisms, the infected person (only in the body) and the antibiotic itself.

The broth dilution method was used to determine the lowest concentration of the ZnONPs that could inhibit the growth of the pathogenic organisms. The MIC for the green synthesized nanoparticle was found to be 100 μg/mL. In a related study,

Ansari et al. (2020) synthesized zinc oxide nanoparticles from Cinnamomum verum plant extract and observed a minimum inhibitory concentration (MIC) of 125 μg/mL and 62.5 μg/mL for *Escherichia coli* and *Staphylococcus aureus* respectively. Furthermore, biosynthesized ZnO–NPs have been found to be effective against plant pathogenic microorganisms such as *Erwinia amylovora, Aspergillus flavus, Aspergillus niger, Fusarium oxysporum, Fusarium moniliform*, and *Alternaria alternata*, with MIC values ranging from 15.6 μg/mL to 500 μg/mL. The percentage of inhibition was observed to increase with an increase in the concentration of the nanoparticle solution. The highest percentage was observed at a concentration of 5000 µg/mL against B. cereus, while the lowest was observed at a concentration of 100 µg/mL against *K. pneumoniae.*

In a similar study, it was reported that the antibacterial activity of ZnONPs increases with an increase in the concentration of ZnONPs due to the increase of H_2O_2 concentration from the surface of ZnONPs. The nanoparticles which were synthesized from Nilgiriantusciliantus leaf extract were observed to inhibit the growth of *Pseudomonas aeruginosa* and *Streptococcus mutans* [37].

Some attempts have been made to explain the mechanism of infiltration of nanoparticles to microbial cells, however, the precise mechanism of interaction between nanoparticles and cell organelles, which initiates antimicrobial activity, is still lacking. Four modes of penetration which includes attachment of the nanoparticles to the cell membrane; the production of Reactive Oxygen Species (ROS) by the Zn ions to damage the microbial DNA; interference of ATP synthesis and DNA replication by the ionic forms of nanoparticles and by interaction with amino acids and nucleic acid moieties as a result of the formation of thiols or phosphates [38]. According to Liu et al [39]., when E. coli was treated with zinc oxide nanoparticles, the particles adhered to the cell membrane, producing membrane deformation and disarray of intracellular structures. The antibacterial effect of zinc oxide nanoparticles on multidrug-resistant S. aureus was examined by Kadiyala et al [40], who concluded that ROS formation alone could not be the predominant antibacterial mode of action. However, one thing is certain: the high amount of zinc ions present at nanoforms disrupts virulence by inhibiting some important glycolytic enzymes due to reduction in hyaluronic acid capsule synthesis, which invariably leads to a shift in the expression of carbon catabolic pathways [41].

Conclusion

In order to limit the use of chemicals in the synthesis of nanoparticles, hexagonal zinc oxide nanoparticles were prepared using the aqueous extracts of plantain peels. The zinc oxide nanoparticles of spherical morphology were characterized for their optical, structural and morphological properties, and the antimicrobial efficacy of the zinc oxide was investigated against different clinical strains of food borne Gram positive and Gram negative bacteria: *Salmonella enterica, Klebsiella pneumoniae, Bacillus cereus* MTCC 430 and *Staphylococcus aureus* 26923, extracted from beef. The biosynthesized nanoparticles exhibited good antimicrobial efficacy against both the Gram-positive and Gram-negative bacteria, with low values of minimum inhibitory concentrations. The study concludes that the synthesis of zinc oxide nanoparticles using the plantain peel extract represents an eco-friendly and cost-effective approach to green ZnO nanoparticles with potent anti- microbial efficiency.

Declaration of Competing Interest

The authors declare no conflict of interest that could have appeared to influence the work reported in this paper.

Funding statement

The reported study was supported by funding from the North-West University and the National Research Foundation, South Africa (Grants Ref: UID117231,UID109333 and UID116338).

References

[1] Z. Obeizi, H. Benbouzid, S. Ouchenane, D. Yılmaz, M. Culha, M. Bououdina, Biosynthesis of Zinc oxide nanoparticles from essential oil of Eucalyptus globulus with antimicrobial and anti-biofilm activities, Mater. Today Commun. 25 (2020) 101553.
[2] A.-L. Välimaa, A. Tilsala-Timisjärvi, E. Virtanen, Rapid detection and identification methods for Listeria monocytogenes in the food chain–a review, Food Control 55 (2015) 103–114.
[3] K. Klaper, J.A. Hammerl, J. Rau, Y. Pfeifer, G. Werner, Genome-based analysis of Klebsiella spp. isolates from animals and food products in Germany, Pathogens 10 (5) (2021) 573.
[4] N. Jessberger, R. Dietrich, P.E. Granum, E. Märtlbauer, The Bacillus cereus food infection as multifactorial process, Toxins (Basel) 12 (11) (2020) 701.
[5] T.O. Ajiboye, S.O. Babalola, D.C. Onwudiwe, Photocatalytic inactivation as a method of elimination of E. coli from drinking water, Appl. Sci. 11 (3) (2021) 1313.
[6] F. Ahmad, M.A. Siddiqui, O.O. Babalola, H.-F. Wu, Biofunctionalization of nanoparticle assisted mass spectrometry as biosensors for rapid detection of plant associated bacteria, Biosens. Bioelectron. 35 (1) (2012) 235–242.
[7] K. Chatfield, B. Salehi, J. Sharifi-Rad, L. Afshar, Applying an ethical framework to herbal medicine, Evid. Complem. Alternat. Med. 2018 (2018) 1903629, doi:10.1155/2018/1903629.
[8] P. Karpecki, M.R. Paterno, T.L. Comstock, Limitations of current antibiotics for the treatment of bacterial conjunctivitis, Optom. Vis. Sci. 87 (11) (2010) 908–919, doi:10.1097/OPX.0b013e3181f6fbb3.
[9] V. Van Giau, S.S.A. An, J.P. Hulme, Mitochondrial therapeutic interventions in Alzheimer's disease, J. Neurol. Sci. 395 (2018) 62–70.
[10] I. Khan, K. Saeed, I. Khan, Nanoparticles: properties, applications and toxicities, Arab. J. Chem. 12 (7) (2019) 908–931, doi:10.1016/j.arabjc.2017.05.011.
[11] C.F. Ajilogba, O.O. Babalola, D.O. Nikoro, Nanotechnology as vehicle for biocontrol of plant diseases in crop production. Edited by OO Babalola, Springer (2021) 709–724, doi:10.1007/978-3-030-50672-8.

[12] T.L. Botha, E.E. Elemike, S. Horn, D.C. Onwudiwe, J.P. Giesy, V. Wepener, Cytotoxicity of Ag, Au and Ag-Au bimetallic nanoparticles prepared using golden rod (Solidago canadensis) plant extract, Sci. Rep. 9 (1) (2019) 4169, doi:10.1038/s41598-019-40816-y.
[13] E.E. Elemike, I.M. Uzoh, D.C. Onwudiwe, O.O. Babalola, The role of nanotechnology in the fortification of plant nutrients and improvement of crop production, Appl. Sci. 9 (3) (2019) 499.
[14] K.K. Bharadwaj, B. Rabha, S. Pati, B.K. Choudhury, T. Sarkar, S.K. Gogoi, N. Kakati, D. Baishya, Z.A. Kari, H.A. Edinur, Green synthesis of silver nanoparticles using diospyros malabarica fruit extract and assessments of their antimicrobial, anticancer and catalytic reduction of 4-Nitrophenol (4-NP), Nanomaterials 11 (8) (2021) 1999.
[15] H.M.M. Ibrahim, Green synthesis and characterization of silver nanoparticles using banana peel extract and their antimicrobial activity against representative microorganisms, J. Radiat. Res. Appl. Sci. 8 (3) (2015) 265–275, doi:10.1016/j.jrras.2015.01.007.
[16] E.E. Elemike, D.C. Onwudiwe, D.F. Ogeleka, E.C. Obasi, Biomediated cellulose-Ag-ZnO nanocomposites and their ecotoxicological assessment using onion bulb plant, J. Cluster Sci. 32 (3) (2021) 651–656, doi:10.1007/s10876-020-01826-3.
[17] P. Pathak, Medicinal properties of fruit and vegetable peels, Adv. Bioeng. (2020) 115–128.
[18] M.A. Ansari, M. Murali, D. Prasad, M.A. Alzohairy, A. Almatroudi, M.N. Alomary, A.C. Udayashankar, S.B. Singh, S.M.M. Asiri, B.S. Ashwini, H.G. Gowtham, N. Kalegowda, K.N. Amruthesh, T.R. Lakshmeesha, S.R. Niranjana, Cinnamomum verum bark extract mediated green synthesis of ZnO nanoparticles and their antibacterial potentiality, Biomolecules 10 (2) (2020) 336.
[19] B.O. Ajiboye, H.O.B. Oloyede, M.O. Salawu, Antihyperglycemic and antidyslipidemic activity of Musa paradisiaca-based diet in alloxan-induced diabetic rats, Food Sci. Nutr. 6 (1) (2018) 137–145, doi:10.1002/fsn3.538.
[20] K.A. Ajijolakewu, A.S. Ayoola, T.O. Agbabiaka, F.R. Zakariyah, N.R. Ahmed, O.J. Oyedele, A. Sani, A review of the ethnomedicinal, antimicrobial, and phytochemical properties of Musa paradisiaca (plantain), Bull. Natl. Res. Centre 45 (1) (2021) 86, doi:10.1186/s42269-021-00549-3.
[21] M.Z. Imam, S. Akter, L. Musa paradisiaca, L. Musa sapientum, A phytochemical and pharmacological review, J. Appl. Pharm. Sci. 1 (5) (2011) 14–20.
[22] A. Pereira, M. Maraschin, Banana (Musa spp) from peel to pulp: ethnopharmacology, source of bioactive compounds and its relevance for human health, J. Ethnopharmacol. 160 (2015) 149–163, doi:10.1016/j.jep.2014.11.008.
[23] E.E. Imade, O.O. Babalola, Biotechnological utilization: the role of Zea mays rhizospheric bacteria in ecosystem sustainability, Appl. Microbiol. Biotechnol. 105 (11) (2021) 4487–4500, doi:10.1007/s00253-021-11351-6.
[24] L. Jiang, G. Sun, Z. Zhou, S. Sun, Q. Wang, S. Yan, Q. Xin, Size-controllable synthesis of monodispersed SnO2 nanoparticles and application in electrocatalysts, J. Phys. Chem. B 109 (18) (2005) 8774–8778, doi:10.1021/jp050334g.
[25] P.S.M. Kumar, A.P. Francis, T. Devasena, Biosynthesized and chemically synthesized titania nanoparticles: comparative analysis of antibacterial activity, J. Environ. Nanotechnol. 3 (3) (2014) 73–81.
[26] A. Phukan, R.P. Bhattacharjee, D.K. Dutta, Stabilization of SnO2 nanoparticles into the nanopores of modified Montmorillonite and their antibacterial activity, Adv. Powder Technol. 28 (1) (2017) 139–145, doi:10.1016/j.apt.2016.09.005.
[27] A. Sirelkhatim, S. Mahmud, A. Seeni, N.H.M. Kaus, L.C. Ann, S.K.M. Bakhori, H. Hasan, D. Mohamad, Review on zinc oxide nanoparticles: antibacterial activity and toxicity mechanism, Nano-Micro Lett. 7 (3) (2015) 219–242, doi:10.1007/s40820-015-0040-x.
[28] P. Sabourian, G. Yazdani, S.S. Ashraf, M. Frounchi, S. Mashayekhan, S. Kiani, A. Kakkar, Effect of physico-chemical properties of nanoparticles on their intracellular uptake, Int. J. Mol. Sci. 21 (21) (2020) 8019.
[29] S.V. Gudkov, D.E. Burmistrov, D.A. Serov, M.B. Rebezov, A.A. Semenova, A.B. Lisitsyn, A mini review of antibacterial properties of ZnO nanoparticles, Front. Phys. 9 (49) (2021), doi:10.3389/fphy.2021.641481.
[30] Z.M. Khoshhesab, M. Sarfaraz, M.A. Asadabad, Preparation of ZnO nanostructures by chemical precipitation method, Synth. React. Inorganic, Met.-Org. Nano-Met. Chem. 41 (7) (2011) 814–819, doi:10.1080/15533174.2011.591308.
[31] P. Samanta, A. Saha, T. Kamilya, Chemical synthesis and optical properties of ZnO nanoparticles, Журнал нано-та електронної фізики (6,№ 4) (2014) 04015-04011-04015-04012.
[32] T. Gur, I. Meydan, H. Seckin, M. Bekmezci, F. Sen, Green synthesis, characterization and bioactivity of biogenic zinc oxide nanoparticles, Environ. Res. 204 (2022) 111897, doi:10.1016/j.envres.2021.111897.
[33] M. Pudukudy, Z. Yaakob, Facile synthesis of quasi spherical ZnO nanoparticles with excellent photocatalytic activity, J. Cluster Sci. 26 (4) (2015) 1187–1201, doi:10.1007/s10876-014-0806-1.
[34] U. El-Nafaty, I. Muhammad, S. Abdulsalam, Biosorption and kinetic studies on oil removal from produced water using banana peel, Civil Environ. Res. 3 (7) (2013) 125–136.
[35] M. Chennimalai, V. Vijayalakshmi, T.S. Senthil, N. Sivakumar, One-step green synthesis of ZnO nanoparticles using Opuntia humifusa fruit extract and their antibacterial activities, Mater. Today: Proc. 47 (2021) 1842–1846, doi:10.1016/j.matpr.2021.03.409.
[36] S. Roy, J.-.W. Rhim, Carrageenan-based antimicrobial bionanocomposite films incorporated with ZnO nanoparticles stabilized by melanin, Food Hydrocoll. 90 (2019) 500–507, doi:10.1016/j.foodhyd.2018.12.056.
[37] M. Arakha, M. Saleem, B.C. Mallick, S. Jha, The effects of interfacial potential on antimicrobial propensity of ZnO nanoparticle, Sci. Rep. 5 (1) (2015) 9578, doi:10.1038/srep09578.
[38] Z. Xia, J. Min, S. Zhou, H. Ma, B. Zhang, X. Tang, Photocatalytic performance and antibacterial mechanism of Cu/Ag-molybdate powder material, Ceram. Int. 47 (9) (2021) 12667–12679, doi:10.1016/j.ceramint.2021.01.127.
[39] Y. Liu, L. He, A. Mustapha, H. Li, Z.Q. Hu, M. Lin, Antibacterial activities of zinc oxide nanoparticles against Escherichia coli O157:H7, J. Appl. Microbiol. 107 (4) (2009) 1193–1201, doi:10.1111/j.1365-2672.2009.04303.x.
[40] U. Kadiyala, E.S. Turali-Emre, J.H. Bahng, N.A. Kotov, J.S. VanEpps, Unexpected insights into antibacterial activity of zinc oxide nanoparticles against methicillin resistant Staphylococcus aureus (MRSA), Nanoscale 10 (10) (2018) 4927–4939, doi:10.1039/C7NR08499D.
[41] V. U Chetan, A systematic review of the interaction and effects generated by antimicrobial metallic substituents in bone tissue engineering, Metallomics 12 (10) (2020) 1458–1479, doi:10.1039/d0mt00127a.